

A Modified Box Model Including Charge Regulation for Protein Adsorption in a Spherical Polyelectrolyte Brush

P. Maarten Biesheuvel^{*,†} and Alexander Wittemann[‡]

Laboratory of Physical Chemistry and Colloid Science, Wageningen University, Dreijenplein 6, 6703 HB Wageningen, The Netherlands, and Lehrstuhl für Physikalische Chemie I, Universität Bayreuth, Universitätsstrasse 30, 95440 Bayreuth, Germany

Received: October 15, 2004; In Final Form: December 1, 2004

Recent experiments showed significant adsorption of bovine serum albumin (BSA) in spherical polyelectrolyte brushes (SPB) consisting of polyacrylic acid, even for pH values above the isoelectric point of the protein, when both protein and polyion are negatively charged. To describe these experimental findings theoretically, we have constructed a spherical box model for an annealed brush consisting of a weak polyelectrolyte that includes the adsorption of BSA. At equilibrium the chemical potential of BSA in solution equals that at each location in the brush, while the net force on the polyions (including osmotic, stretching, and excluded volume terms) is zero at each location. Protein adsorption is predicted above the isoelectric point and—in agreement with experimental data—is a strong function of ionic strength and pH. Adsorption of protein in the brush is possible because the pH in the brush is below the isoelectric point and protein reverses its charge from negative to positive when it adsorbs.

Introduction

The interaction of protein molecules with surfaces is important in many biological problems and technological applications.^{1–7} Protein adsorption must often be avoided (bio-fouling), while many technologies require immobilization of proteins and enzymes without reduction in activity.

Colloidal particles represent excellent model systems for the investigation of the adsorption of molecules from solution as they provide large surface areas. In recent studies, it was shown that colloidal particles modified by grafting long, densely packed polyelectrolyte chains provide a new class of immobilization agent with interesting properties.^{8–11} These spherical polyelectrolyte brushes (SPB), consisting of a polystyrene core of ~100 nm diameter onto which long chains of polyacrylic acid are anchored,¹² are able to adsorb large amounts of protein (up to 1 g per g of SPB) as long as the ionic strength is low enough.^{8,9} However, when the ionic strength or pH is increased the protein molecules are released into solution.⁹ Therefore reversible loading and deloading of the SPB with protein molecules is possible and the system may serve as an enzymatic nanoreactor.⁹

Interestingly, the adsorption experiments could be carried out at a pH where the protein molecules are like-charged to the substrate,⁸ which is surprising because an electrostatic repulsion is expected between like-charged materials. As experiments showed that the counterions of the polyelectrolyte chains are confined within the brush layer,^{13,14} Wittemann et al.⁸ and Czeslik et al.¹⁵ suggested that upon protein adsorption “counterion evaporation” (from within the brush and from the protein molecules) leads to an increase in entropy, which serves as the driving force of the protein adsorption process.

In the present work we will also discuss electrostatic free energies at the Poisson–Boltzmann level, but discuss in more detail the ionizable properties of the amphoteric protein

molecule. Indeed, during adsorption the ionization of the different types of amino acid residues changes because of the different local pH.^{16,17} Near a negatively charged surface the pH is lower than in bulk solution and protein molecules that are negatively charged in solution may reverse their charge when they adsorb. Note that throughout this paper, pH is used as a measure of proton concentration, not of the chemical potential of the protons in the system—which at equilibrium is equal throughout the system.

To analyze protein adsorption in a SPB we will set up a spherical ionizable polyelectrolyte brush model along the lines of planar brush “Alexander-De Gennes” box models, with the adjustments suggested (for a neutral brush) by Borisov and Zhulina¹⁸ to make such models applicable to a spherical geometry. At each radial coordinate in the spherical brush electroneutrality is assumed with the electroneutrality balance having contributions from the SPB, small ions, and adsorbed protein. In reality local electroneutrality becomes only correct deep inside the brush layer (when grafted on a neutral interface) while a charge separation develops between the periphery of the brush and the diffuse ion cloud extending from the brush.

The ionization of both the SPB and the amino acid residues is a self-consistent function of the local electrostatic potential, and is therefore a function of brush coordinate. Adsorbed protein molecules are at equilibrium with those in solution, where we envision a spherical ion cloud around the (assumed spherical) protein molecules. We assume in the calculations that all polymer chains are of equal length (monodisperse) though in reality polydispersity effects are important.

The adsorption of protein in neutral brushes was discussed by Currie et al.⁷ (and references therein) using a mean-field box model. To describe the interaction of protein with charged brushes, in ref 15 the interaction energies of an (assumed planar) protein surface with a homogeneous brush phase was analyzed. To our understanding the present paper is the first in which the adsorption of protein in charged brushes is described using a

* Corresponding author. E-mail: maarten.biesheuvel@wur.nl.

† Wageningen University.

‡ Universität Bayreuth.

brush model including charge regulation. Both in Theory and in the Results and Discussion we will discuss the spherical ionizable polyelectrolyte brush model first, followed by an analysis of protein adsorption in a SPB.

Theory

Spherical Ionizable Polyelectrolyte Brush. The spherical polyelectrolyte brush model is an extension of the neutral spherical brush model by Borisov and Zhulina.¹⁸ In the (spherical) box model all chains behave identically, all being equally stretched at each radial coordinate r (the degree of stretching is a function of r). Consequently, all free ends are located at the same distance away from the core particle, namely at the edge of the brush. At each radial coordinate the force on the polyions is set to zero. By integrating across the brush it is possible to derive analytical expressions for the thickness of a neutral brush.¹⁸ For ionizable polyelectrolytes we do not aim at analytical expressions but solve the box model numerically. We incorporate the charges on the polyelectrolyte chains and assume local electroneutrality (at each r). The force on the polyions includes conformational entropy (stretching), excluded volume (mixing, or concentration terms), and electrostatic/osmotic forces.

For the conformational contribution we use Gaussian elasticity and include the elastic overstretching term introduced by Lyulin et al.¹⁹ (see also ref 20), which results for the conformational force on a polyelectrolyte chain in

$$f_{\text{conf}} = -\frac{1}{k} \left(3x - \frac{27}{20} x^2 \ln(1-x) + \frac{9}{20} \frac{x^3}{1-x} \right) \quad (1)$$

which starts to underestimate the correct elastic contribution above 85% stretching, but (correctly) goes to minus infinity for $x \rightarrow 1$ (a negative force is contractive). In eq 1, k is the Kuhn length and x the degree of stretching ($0 < x < 1$). Alternatively, we could have implemented in the numerical model the exact solution instead, which is $x = 1/\tanh(k \cdot f_{\text{conf}}) - 1/(k \cdot f_{\text{conf}})$.

Based on Flory–Huggins mean field theory the contribution to the free energy density because of mixing chains and solvent, F_{conc} , is

$$F_{\text{conc}} \nu_{\text{FH}} = (1 - \phi) \ln(1 - \phi) + \chi \phi(1 - \phi) \quad (2)$$

where ϕ is the polymer volume fraction and ν_{FH} is the Flory–Huggins lattice site volume, which is not necessarily equal to the volume of a brush monomer, ν_b . Throughout this paper we use ν_b for the volume of a segment (or, monomer) of the brush chains; ν_p is the volume of the protein molecule. In eq 2 we have assumed the polymerization degree N to be large enough that the term $\phi/N \ln \phi$ can be neglected. Typically, eq 2 is linearized for the low- ϕ regime to obtain the force, f , on a chain (based on $f = -1/\sigma \, dHF/dH$ with H the brush height, and $\sigma N \nu_b = \phi H$)

$$f_{\text{conc}} = \frac{\nu}{2\nu_{\text{FH}}} \frac{\phi^2}{\sigma} \quad (3)$$

with ν the second virial coefficient, $1 - 2\chi$, and σ the local grafting density (in m^{-2}). In the present work, we do not linearize eq 2, while we neglect hydrophobic interactions and thus assume $\chi = 0$. In this case, eq 2 results in

$$f_{\text{conc}} = -\frac{\phi + \ln(1 - \phi)}{\nu_{\text{FH}} \sigma} \quad (4)$$

where we use ν_{FH} as a fitting parameter instead of the virial coefficient ν . The advantage of eq 4 over eq 3 is that f_{conc} (correctly) goes to infinity when $\phi \rightarrow 1$.

For a spherical brush, only the grafting density at the interface with the underlying core particle, σ_0 at R (R being the radius of the core particle), is known a priori. The local grafting density $\sigma(r > R)$ is given by

$$\sigma = \sigma_0 \frac{R^2}{r^2} \quad (5)$$

Local electroneutrality at each location r in the brush requires

$$\frac{\phi_b}{\nu_b} z \alpha_b - 2n_{\infty} \sinh y(1 - \phi) = 0 \quad (6)$$

where we assume that each segment carries one ionizable charge. In eq 6 z is the charge sign ($z = -1$ for an anionic polyelectrolyte), α_b the ionization degree of the brush polyelectrolyte, n_{∞} the ionic strength in bulk solution (in m^{-3}), and y the local dimensionless electrostatic potential. Based on a Langmuir adsorption isotherm, α depends on y according to^{17,20}

$$\alpha = \frac{1}{1 + 10^{z(\text{pH}_{\infty} - \text{pK})} e^{zy}} = \frac{1}{1 + 10^{z(\text{pH}_1 - \text{pK})}} \quad (7)$$

where pK is the intrinsic pK value, a thermodynamic number dependent on the proton adsorption energy, pH_{∞} is the pH in bulk solution, and pH_1 is the local pH. The bulk pH, pH_{∞} , and local pH, pH_1 , are related via Boltzmann: $\text{pH}_1 = \text{pH}_{\infty} + y/\ln(10)$. Again, pH as used in this paper is a measure of proton concentration, not chemical potential; thus, it can have different values at different locations within a system at chemical equilibrium. In eq 6 we have included a term “ $1 - \phi$ ” that describes the fact that polymer excludes volume for solvent and small ions. This term was suggested in ref 20 and has been used at length in ref 21. Having solved for α and y , the osmotic/electrostatic force on the polyions is given by²⁰

$$f_{\text{osm}} = \frac{2n_{\infty}}{\sigma} (\cosh y - 1) \quad (8)$$

Equation 8 is valid in a box model with local electroneutrality assumed, irrespective of the use of the term “ $1 - \phi$ ” in the electroneutrality balance, or the presence of protein in the brush. At each radial coordinate the sum of forces on a polyion equals zero,

$$f_{\text{conf}} + f_{\text{conc}} + f_{\text{osm}} = 0 \quad (9)$$

The above set of equations can be solved together with conservation of polyion mass,

$$Na = \int_R^D \frac{1}{x} dr \quad (10)$$

where a is the monomer segment length and D the radial coordinate at the outermost dimension (“edge”) of the brush.

Protein in Solution. We describe the protein molecule in solution as a sphere of radius b with a homogeneous surface charge, Z_{∞} . To simplify the solution of the Poisson–Boltzmann equation, we use a spherical (Wigner–Seitz) cell model²² in which we assume the protein molecules to be homogeneously distributed, and envision a spherical cell around each molecule. Each cell contains one protein molecule and a certain volume of solution phase (containing the small ions). All cells together

fill the total volume and thus the protein volume fraction ϕ_∞ relates to the sphere radius, b , and the cell radius, c , according to $\phi_\infty = b^3/c^3$. Each cell is electroneutral, thus the charge of the small ions in each cell exactly compensates the surface charge on the molecule. At the edge of the cell the gradient in potential, dy/dr , is zero, but not the potential, y_c , which is zero at infinite dilution only.

The cell model uses the Poisson–Boltzmann equation in spherical coordinates in the low potential (Debye–Hückel) limit, given by

$$\frac{1}{r^2} \frac{d}{dr} r^2 \frac{dy}{dr} = \kappa^2 y \quad (11)$$

We solve eq 11 in the annular space $b < r < c$ with the two boundary conditions

$$\begin{aligned} r = b: \quad \frac{dy}{dr} &= -\frac{Z_\infty \lambda_B}{b^2} \\ r = c: \quad \frac{dy}{dr} &= 0 \end{aligned} \quad (12)$$

resulting in

$$\frac{Z_\infty \lambda_B}{b^2} = \kappa \left(\chi + \frac{1}{\kappa b} \right) y_\infty \quad (13)$$

with the parameter χ given by

$$\chi = 1 - 2 \left(1 + \frac{\kappa b \phi_\infty^{-1/3} - 1}{\kappa b \phi_\infty^{-1/3} + 1} \exp(2\kappa b(\phi_\infty^{-1/3} - 1)) \right)^{-1} \quad (14)$$

where y_∞ is the dimensionless electrostatic potential at the surface of the protein molecule (at $r = b$), ϕ_∞ the volume density of protein in solution, κ the inverse of the Debye length, $\kappa^2 = 2e^2 n_\infty / (\epsilon kT)$, when all ions are monovalent (ionic strength, or salt concentration, is $n_\infty = c_\infty N_{av}$ with c_∞ in mM), k the Boltzmann constant, T temperature, e the electronic charge, N_{av} Avogadro's number, ϵ the dielectric constant (in water $78 \times 8.854 \times 10^{-12}$ F/m), and λ_B the Bjerrum length, given by $\lambda_B = e^2 / (4\pi\epsilon kT)$. When $\phi \rightarrow 0$, $\chi \rightarrow 1$ and eq 13 simplifies to the well-known expression for an isolated spherical double layer^{16,17,23}

$$\frac{Z_\infty \lambda_B}{b} = (1 + \kappa b) y_\infty \quad (15)$$

In a spherical cell model the electrostatic contribution to the osmotic pressure is (Debye–Hückel limit)

$$\Pi = n_\infty y_c^2 = \frac{\lambda_B b \phi_\infty^{2/3}}{6v_p} \left[\frac{Z_\infty \kappa \exp(\kappa b(\phi_\infty^{-1/3} - 1))(1 - \chi)}{(\kappa b \phi_\infty^{-1/3} + 1) \left(\chi + \frac{1}{\kappa b} \right)} \right]^2 \quad (16)$$

where y_c is the electrostatic potential at the edge of the cell, and v_p is the volume of the spherical protein molecule.

We describe BSA using the classical titration model²³ but use a simplification¹⁷ by considering only a fixed positive charge, q_f (containing all cationic lysine and arginine residues, for which $\alpha = 1$ is assumed, minus adsorbed chloride), and ionizable anionic, q_- , and cationic sites, q_+ , which results for Z in

$$Z = q_f - q_- \alpha_- + q_+ \alpha_+ \quad (17)$$

Using $q_f = 73$, $q_- = 100$, $q_+ = 16$, $pK_- = 4.2$ (aspartic acid, glutamic acid), and $pK_+ = 6.9$ (histidine) an isoelectric point, pI , of 5.1 results. The ionization degrees, α_- and α_+ , follow from eq 7 with $z_+ = 1$ and $z_- = -1$.

In general, the chemical potential, μ , of a certain molecule (of volume v_p) is related to the osmotic pressure Π according to²⁴

$$\mu = F^* + \frac{v_p}{\phi} \Pi \quad (18)$$

where F^* is the free energy per molecule. The electrochemical contribution to F^* in the Debye–Hückel limit is given by^{20,25}

$$F^* = \left(q_f - \frac{1}{2} Z_\infty \right) y_\infty + \sum_{i=+, -} q_i \ln(1 - \alpha_{i,\infty}) \quad (19)$$

Combination of eqs 16, 18, and 19 results in the electrochemical contribution to the chemical potential of the protein molecules

$$\begin{aligned} \mu = & \left(q_f - \frac{1}{2} Z_\infty \right) y_\infty + \sum_{i=+, -} q_i \ln(1 - \alpha_{i,\infty}) + \frac{\lambda_B b}{6\phi_\infty^{-1/3}} \\ & \left[\frac{Z_\infty \kappa \exp(\kappa b(\phi_\infty^{-1/3} - 1))(1 - \chi)}{(\kappa b \phi_\infty^{-1/3} + 1) \left(\chi + \frac{1}{\kappa b} \right)} \right]^2 \end{aligned} \quad (20)$$

with the summation running over the two types of ionizable sites.

Equations 19 and 20, and eqs 23 and 26 to be discussed further on, contain chemical contributions to μ and F which stem from adsorption and desorption of protons to/from the amino acid residues of the protein molecules.^{16,20,25} The chemical contribution contains two elements. The first is due to the energy of proton adsorption (negative for a cationic residue, positive for an anionic residue), and is directly related to the intrinsic pK value of the specific amino acid. The second element is the entropy related to the mixing of neutral and ionized states of the molecule. Chemical energy is released when an ionizable group increases its charge (more positive for a cationic charge; more negative for an anionic charge). When a protein molecule moves into the brush chemical energy is released, first because of the brush polyions that are able to charge up further and, second, because of the increasing charge of the cationic amino acid residues; however, the anionic amino acids reduce their charge, which is energetically unfavorable.

The second contribution to μ is translational entropy. Here we use Carnahan–Starling, which results in²⁶

$$\mu = \ln \phi_\infty + \frac{\phi_\infty(8 - 9\phi_\infty + 3\phi_\infty^2)}{(1 - \phi_\infty)^3} \quad (21)$$

Summation of eqs 20 and 21 gives the total chemical potential of a protein molecule in solution, μ_∞ .

Protein Adsorption in Polyelectrolyte Brush. When protein adsorbs in the brush, eq 6 must be modified to include the charges due to the protein, and the volume excluded for small ions. These modifications result in

$$-\frac{\phi_b}{v_b} \alpha_b + Z \frac{\phi_p}{v_p} - 2n_\infty \sinh y(1 - \phi_b - \phi_p) = 0 \quad (22)$$

where we have assumed a polyanionic brush. For the brush, the volume fraction is ϕ_b , and for the protein, ϕ_p . The parameters Z , y , ϕ_b , and ϕ_p are all functions of the radial coordinate, r .

In the excluded volume contribution to the force on a polyion, f_{conc} given by eq 4, we neglect the influence of protein, and use ϕ_b for ϕ . Equally, for the entropy of the protein in the brush, based on eq 21, ϕ_p is used, thereby neglecting the influence of the brush polyions on the entropy of the protein molecules.

At each location in the brush the chemical potential of a protein molecule, μ , is equal to the bulk value, μ_∞ . The chemical potential has an entropic contribution (eq 21 with ϕ_∞ replaced by ϕ_p), while the electrochemical contribution to μ in the brush is given by

$$\mu = q_F y + \sum_{i=+,-} q_i \ln(1 - \alpha_i) + 2n_\infty v_p (\cosh y - 1) \quad (23)$$

Equation 23 is the correct expression for the electrochemical contribution given eq 22. This implies that (1) all small ions are monovalent, (2) the volume of the protein molecule is implemented in eq 22, and (3) electrostatic potential gradients are neglected and, thus, at each coordinate r the brush is electroneutral. The first term of eq 23 is the typical expression for a charge q_F of zero volume in a mean field, the second term relates to the ionizable groups of the molecule, and the third term describes the fact that a protein molecule excludes volume for solvent and small ions.

Alternatively, we can obtain the chemical potential of the protein molecules, μ , numerically from

$$\mu = v_p \left. \frac{dF}{d\phi_p} \right|_{\phi_b} \quad (24)$$

that is, as the derivative of the local free energy density in the brush F with volume fraction of protein, ϕ_p , for a constant volume fraction of the brush polyions, ϕ_b . As μ is obtained for constant ϕ_b , the concentration and conformation terms for the polyions, eqs 1–4, do not need to be considered here. The entropic contribution for the protein follows from eq 21 with ϕ_∞ replaced by ϕ_p . The electrochemical contribution to the free energy density in the brush, F , is obtained numerically from evaluating eq 22 and related electrostatic equations at a dummy density, ϕ'_p , marginally different from ϕ_p (but with constant ϕ_b), and by making use of

$$\mu = v_p \frac{F - F'}{\phi_p - \phi'_p} \quad (25)$$

Assuming electroneutrality at each location in the brush, eq 22, the electrochemical contribution to the free energy density, F , is given by^{16,17,20}

$$F = -\frac{\phi_b}{v_b} \ln(1 - \alpha_b) + \frac{\phi_p}{v_p} [q_F y + \sum_{i=+,-} q_i \ln(1 - \alpha_i)] - 2n_\infty (\cosh y - 1) (1 - \phi_b - \phi_p) \quad (26)$$

The analytical expression, eq 23, gives exactly the same result as the numerical procedure based on eqs 25 and 26.

Results and Discussion

Spherical Polyelectrolyte Brush. For polyacrylic acid we use a monomer segment length, a , of 0.25 nm, and a segment radius of 0.3 nm, which results in a monomer volume, v_b , of 0.071 nm³. The brush thickness, $L = D - R$, was presented as

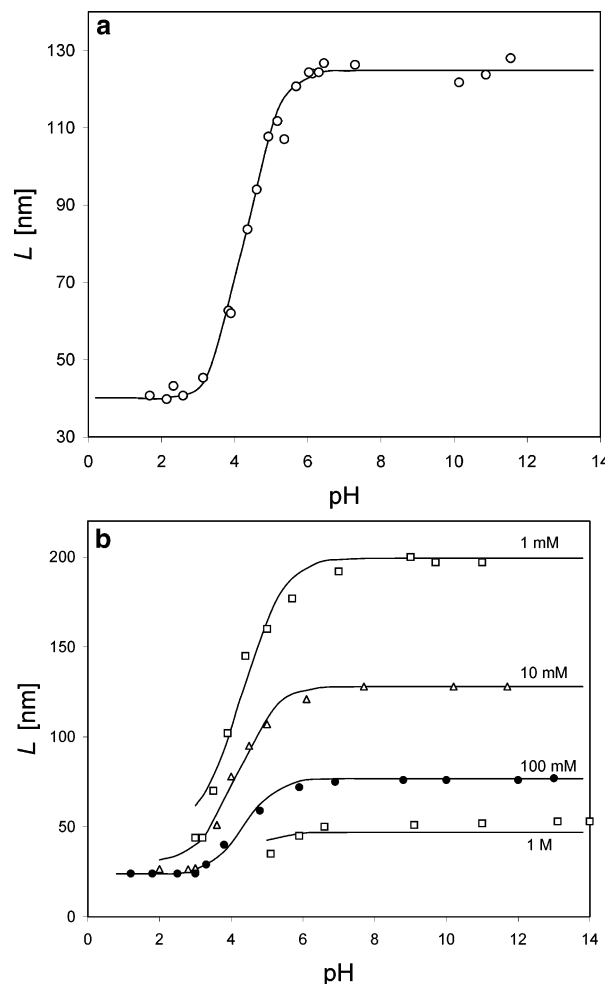


Figure 1. Thickness of ionizable spherical polyelectrolyte brush. (a). Ionic strength 80 mM. Data from ref 8 (system L16). Fitted parameters: $v_{FH} = 0.057 \text{ nm}^3$, $k = 1 \text{ nm}$, $pK = 4.2$. (b). Data from ref 12 (system L15).

function of pH for 80 mM ionic strength in Figure 3 of ref 8. (System L16, $R = 54 \text{ nm}$, $L_c = Na = 209 \text{ nm}$, $\sigma_0 = 0.054 \text{ nm}^{-2}$; all contour lengths mentioned in this work are number averages. Note that in ref 8 it was erroneously mentioned that the ionic strength was 10 mM in this experiment.)

The data and a model calculation are presented in Figure 1a. Making the comparison allows us to determine each of the three fitting parameters: Kuhn length k , pK , and v_{FH} . Fitting the brush thickness at high pH results in a value for the Kuhn length of 4 times the segment length, thus $k = 1 \text{ nm}$. From the minimum at low pH we derive $v_{FH} = 0.8v_b$. The curve is shifted left-right by adjusting pK . An optimum value is $pK = 4.2$ for the carboxylic groups (just as will be used for the carboxylic groups of the protein).

Data at different ionic strengths were given for system L15 ($R = 66 \text{ nm}$, $L_c = 228 \text{ nm}$, $\sigma_0 = 0.039 \text{ nm}^{-2}$) in Figure 3 of ref 12 and are reproduced in Figure 1b. Calculation results in Figure 1b are based on $v_{FH} = 0.8v_b$ for each value of the ionic strength. However, both the Kuhn length k and pK depend on the ionic strength. The Kuhn length increases with increasing polyion line charge and electrostatic potential. The electrostatic potential in turn increases with increasing grafting density and Debye length λ_D (lower ionic strength). The pK values can be different between curves as well: with increasing ionic strength diffuse layers around individual chains overlap less, and the potential change over the diffuse layer increases. Therefore the ionization

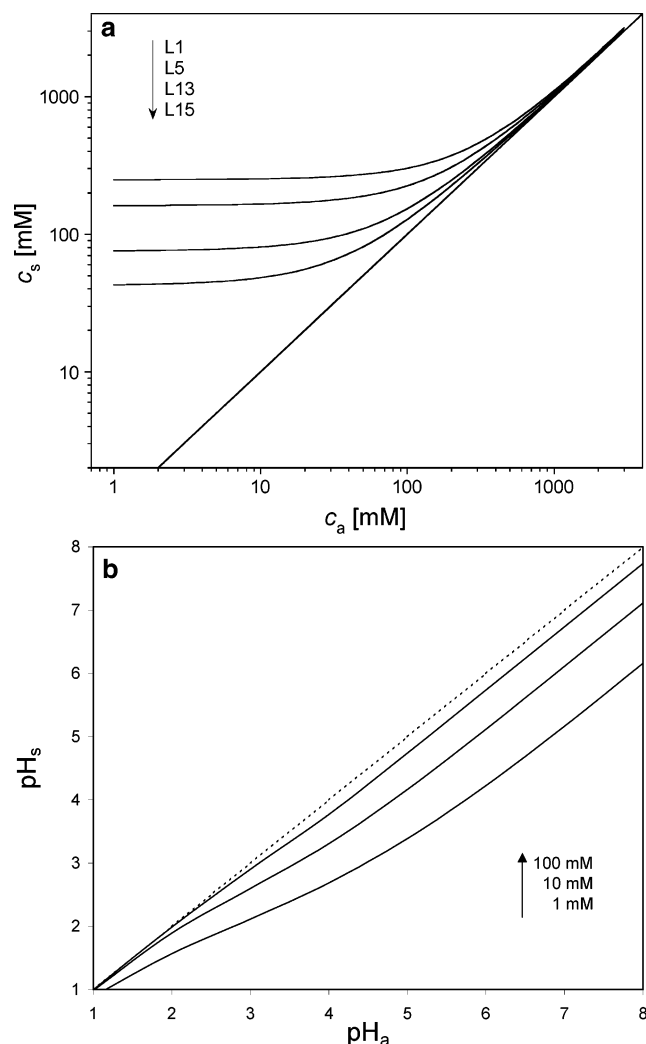


Figure 2. Ionic strength (c_s) and pH in the brush (pH_s) as a function of external conditions (c_a , pH_a). (a). systems L1, L5, L13, and L15 of ref 12. (b). pH inside the brush layer as a function of bulk pH (system L16 of Figure 1a).

degree of the chain decreases compared to a flat y -profile and the thickness–pH curve shifts to the right. To correct this in a box model (where the variation of y is neglected) pK must be increased with increasing ionic strength. Indeed, fitting the model to the data resulted in a decreasing Kuhn length and increasing pK with increasing ionic strength: for 1 mM, $k = 1.62$ nm and $pK = 3.5$; for 10 mM, $k = 0.36$ nm and $pK = 3.5$; for 100 mM, $k = 0.16$ nm and $pK = 4$; and for 1 M, $k = 0.16$ nm and $pK = 4.2$.

The model can be used to calculate the effective ionic strength in the brush, c_s , as a function of ionic strength in bulk solution, c_a , as calculated for high pH (>8) in refs 12 and 27—ionic strength in the brush here defined as half of the total local small ion concentration, thus actually equal to $c_a \cosh(y)$ (under these conditions of high pH the brush is quite expanded, ϕ low, and the term $1 - \phi$ can be neglected). To obtain c_s (via y) from the calculation, one should either average over the brush or choose a representative location within the brush. We use the latter option and evaluate y and c_s at r where the exact middle of each brush polyion is located. Figure 2a shows results for the four spherical brush systems used in Figure 5 of ref 12, namely L1 ($R = 99$ nm, $L_c = 36$ nm, $\sigma_0 = 0.062$ nm $^{-2}$), L5 ($R = 55$ nm, $L_c = 55$ nm, $\sigma_0 = 0.057$ nm $^{-2}$), L13 ($R = 54$ nm, $L_c = 134$ nm, $\sigma_0 = 0.050$ nm $^{-2}$), and L15 ($R = 66$ nm, $L_c = 228$

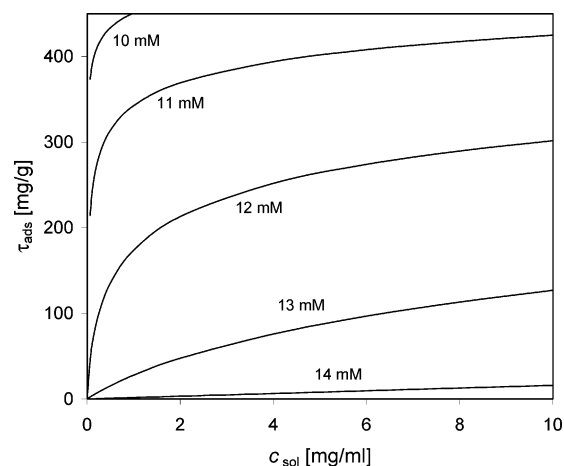


Figure 3. Model calculations for BSA adsorption in a spherical polyelectrolyte brush as a function of BSA concentration in solution and of ionic strength (pH 5.6, system KpS13 of ref 8; $\sigma = 0.13$ nm $^{-2}$, $R = 51$ nm, contour length $Na = 36$ nm).

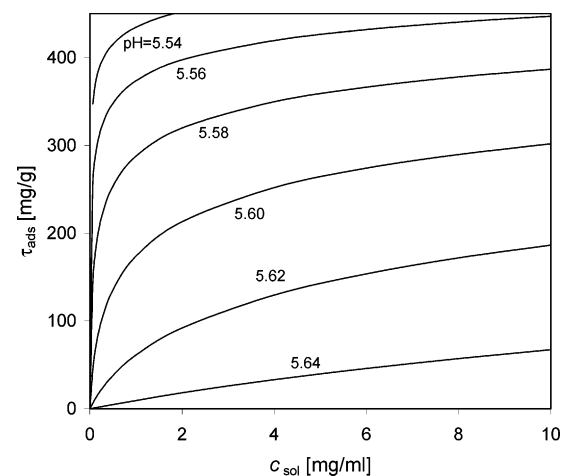


Figure 4. Model calculations for BSA adsorption in a spherical polyelectrolyte brush as a function of BSA concentration in solution and of pH (ionic strength 12 mM, system KpS13, see Figure 3).

nm, $\sigma_0 = 0.039$ nm $^{-2}$). There is a close agreement with earlier calculations with the same change in c_s as a function of the chosen system, and of c_a .¹² The same model also allows calculation of pH in the brush, pH_s , as a function of pH in bulk solution, pH_a , see Figure 2b. With decreasing ionic strength the pH difference between brush and solution increases strongly (lower pH in brush), which makes charge reversal of adsorbed protein molecules possible.

Protein Adsorption in Spherical Ionizable Polyelectrolyte Brush. Next, we present calculation results for the adsorption of BSA in a polyelectrolyte brush as a function of protein concentration in solution, c_{sol} , pH, and ionic strength (system KpS13 of ref 8, $\sigma_0 = 0.13$ nm $^{-2}$, $R = 51$ nm, $Na = 36$ nm). We assume a volume for the BSA molecule of $v_p = 163$ nm 3 (MW = 67 kDa).²⁸ For the SPB, we will use the values for v_{FH} , k , and pK derived in Figure 1a.

To calculate τ_{ads} , the adsorbed amount of BSA per gram of spherical brush particles, we assume that the polystyrene core ($\rho = 1.06$ g/cm 3) of radius $R = 51$ nm completely determines the mass of the colloidal particle. Figure 3 shows the influence of protein concentration in solution, c_{sol} , and ionic strength, on τ_{ads} and can be compared to the experimental data of Figure 6 in ref 8. Figure 4 shows the influence of c_{sol} and pH for a given ionic strength, comparable to Figure 8 of ref 8.

Comparing calculation results with the data we find a qualitative agreement: adsorbed amounts are roughly in the same range and the influence of solution concentration, pH, and ionic strength is qualitatively reproduced by the model. Most importantly, the model indeed predicts protein adsorption in a like-charged brush, with increasing amounts of adsorption with increasing c_{sol} and decreasing pH or ionic strength. In line with the experiments, at the more unfavorable conditions for adsorption (high pH, high ionic strength) the model correctly predicts a linear dependence of τ_{ads} on c_{sol} , while for more favorable conditions the adsorption τ_{ads} first rapidly increases and then starts to level off.

However, the model significantly overestimates the sensitivity of the adsorbed amount to pH and ionic strength, while an observed “upswing” in adsorbed amount at high c_{sol} is not reproduced either. One obvious reason for such discrepancies is the absence in the model of nonelectrostatic interaction energies between the different molecules. Hydrophobic forces might moderate the predicted influence of pH and ionic strength, while a protein–protein attractive component might lead to enhanced adsorption above a certain protein concentration leading to the observed upswing in adsorption at high c_{sol} .

Besides, the discrepancies may be due to the assumption underlying the box model that all free ends are located at the edge of the brush. In reality, the brush density decreases much more gradually with radial coordinate than the block profile predicted by the box model. The gradual decrease is augmented by the polydispersity in the length of the polyelectrolyte chains, which is not considered in the box model either. Consequently, in the periphery of the brush the SPB density is low and the mean-field approach less appropriate: though deep inside the brush the protein molecule experiences a homogeneous electrostatic environment and interacts on all sides with many chains simultaneously, in the periphery of the brush layer the protein molecules interact only with individual chains and it is possible for a net negative, but dipolar, molecule to adsorb to a negative chain by orienting the negative pole away. Such a mechanism, based on the patchiness of the charge distribution on a protein molecule, might influence the adsorbed amount of protein, especially for a low Debye length and/or low brush density.

Despite these concerns, it can certainly be concluded that electrostatic forces play a decisive role in the adsorption of protein in a polyelectrolyte brush.¹⁵ More specifically, the amphoteric character of the protein molecules and the resulting charge reversal upon adsorption is a key element of the adsorption process.

Conclusions

A spherical box model is set up for an ionizable polyelectrolyte brush. Stretching is described including an overstretching term, and mixing energies without making the assumption of a dilute brush. In the electroneutrality balance volume exclusion by the polymer is included, reducing the volume available to the small ions. The model describes data in the absence of protein for the brush thickness as a function of pH and ionic strength, and predicts pH and ionic strength in the brush.

Upon adsorption, protein molecules throughout the brush regulate their charge and are at thermodynamic equilibrium with

each other and with molecules in solution. In full accordance with the experimental data the model predicts that protein adsorption in a like-charged brush is possible—according to the model because of charge reversal of the amphoteric protein molecule. Charge reversal is most likely at pH still close to the isoelectric point and at a low ionic strength. Under these circumstances protein and brush serve as each others counterions. With increasing ionic strength or pH, however, it becomes more favorable for the small ions to take over the role of counterion, both for the polyacrylic acid brush and for the protein molecules in solution, resulting in a decrease in protein adsorption.

Acknowledgment. This research was financially supported by NWO, Netherlands Organisation for Scientific Research.

References and Notes

- (1) Hartmeier, W. *Immobilisierte Biokatalyse: Eine Einführung*, Springer-Verlag: Dusseldorf, Germany, 1986.
- (2) *Proteins at Interfaces: Fundamentals and Applications*; Horbett, T. A., Brash, J. L., Eds.; ACS Symp. Ser. No. 602; American Chemical Society: Washington, DC, 1995.
- (3) Halperin, A. *Langmuir* **1999**, *15*, 2525.
- (4) Kawaguchi, H. *Prog. Polym. Sci.* **2000**, *25*, 1171.
- (5) Bru-Rovira, M.; Giralt, F.; Cohen, Y. *J. Colloid Interface Sci.* **2001**, *235*, 70.
- (6) Azioune, A.; Chehimi, M. M.; Miksa, B.; Basinska, T.; Slomkowski, S. *Langmuir* **2002**, *18*, 1150.
- (7) Currie, E. P. K.; van der Gucht, J.; Borisov, O. V.; Cohen Stuart, M. A. *Pure Appl. Chem.* **1999**, *71*, 1227.
- (8) Wittemann, A.; Haupt, B.; Ballauff, M. *Phys. Chem. Chem. Phys.* **2003**, *5*, 1671.
- (9) Wittemann, A.; Ballauff, M. *Anal. Chem.* **2004**, *76*, 2813.
- (10) Neumann, Th.; Haupt, B.; Ballauff, M. *Macromol. Biosci.* **2003**, *4*, 13.
- (11) Czeslik, C.; Jackler, G.; Hazlett, T.; Gratton, E.; Steitz, R.; Wittemann, A.; Ballauff, M. *Phys. Chem. Chem. Phys.* **2004**, *6*, 5557.
- (12) Guo, X.; Ballauff, M. *Langmuir* **2000**, *16*, 8719.
- (13) Das, B.; Guo, X.; Ballauff, M. *Prog. Colloid Polym. Sci.* **2002**, *121*, 34.
- (14) Dingenouts, N.; Merkle, R.; Guo, X.; Narayanan, T.; Goerigk, G.; Ballauff, M. *J. Appl. Crystallogr.* **2003**, *36*, 578.
- (15) Czeslik, C.; Jackler, G.; Steitz, R.; von Grünberg, H.-H. *J. Phys. Chem. B* **2004**, *108*, 13395.
- (16) Biesheuvel, P. M.; van der Veen, M.; Norde, W. *J. Phys. Chem. B* **2005**, *109*, 4172.
- (17) Biesheuvel, P. M.; Stroeve, P.; Barneveld, P. *J. Phys. Chem. B* **2004**, *108*, 17660.
- (18) Borisov, O. V.; Zhulina, E. B. *Macromolecules* **2003**, *36*, 10029.
- (19) Lyulin, S. V.; Evers, L. J.; van der Schoot, P.; Darinskii, A. A.; Lyulin, A. V.; Michels, M. A. J. *Macromolecules* **2004**, *37*, 3049.
- (20) Biesheuvel, P. M. *J. Colloid Interface Sci.* **2004**, *275*, 97.
- (21) Ahrens, H.; Förster, S.; Helm, C. A.; Kumar, N. A.; Naji, A.; Netz, R. R.; Seidel, C. *J. Phys. Chem. B* **2004**, *108*, 16870.
- (22) Alexander, S.; Chaikin, P. M.; Grant, P.; Morales, G. J.; Pincus, P. *J. Chem. Phys.* **1984**, *80*, 5776.
- (23) Pujar, N. S.; Zydney, A. L. *J. Colloid Interface Sci.* **1997**, *192*, 338.
- (24) Russel, W. B.; Saville, D. A.; Schowalter, W. R. *Colloidal Dispersions*; Cambridge University Press: New York, 1989.
- (25) Borisov, O. V.; Boulakh, A. B.; Zhulina, E. B. *Eur. Phys. J. E* **2003**, *12*, 543.
- (26) Vliegthart, G. A.; Lekkerkerker, H. N. W. *J. Chem. Phys.* **1999**, *111*, 4153.
- (27) Hariharan, R.; Biver, C.; Russel, W. B. *Macromolecules* **1998**, *31*, 7514.
- (28) González Flecha, F. L.; Levi, V. *Biochem. Mol. Biol. Edu.* **2003**, *31*, 319.